Unimolecular Chemistry of Ionized Vinylamine, $[CH_2CHNH_2]^{\bullet+}$: A Mass Spectrometric and Molecular Orbital Study

Guy Bouchoux,*,† Florence Penaud-Berruyer,† and Minh Tho Nguyen‡

Contribution from the Departement de Chimie, Laboratoire des Mécanismes Réactionnels, Ecole Polytechnique, F91128 Palaiseau, France, and Department of Chemistry, University of Leuven, Celestijnenlaan 200F, B-300-Leuven, Belgium

Received May 10, 1993®

Abstract: Isomerization and dissociation of the vinylamine radical cation $[CH_2{=}CHNH_2]^{\bullet+}$ ($\mathbf{1}^{\bullet+}$) was explored by using both mass spectrometric techniques and molecular orbital calculations. The ground-state potential energy surface of $[C_2H_5N]^{\bullet+}$cations containing the CCN frame was examined by ab initio molecular orbital calculations terminated at the PUMP4/6-311++G**//MP2/6-31G**+ZPE level. The global minimum corresponds to the vinylamine radical cation $[CH_2{=}CHNH_2]^{\bullet+}$ ($\mathbf{1}^{\bullet+}$), which is 81 and 122 kJ/mol more stable than $[CH_3CNH_2]^{\bullet+}$ ($\mathbf{2}^{\bullet+}$) and $[CH_3CHNH]^{\bullet+}$ ($\mathbf{3}^{\bullet+}$) ions, respectively. Isomerization and dissociation of $\mathbf{1}^{\bullet+}$ into $[C_2H_4N]^+ + H^\bullet$ were evaluated in detail. It is demonstrated that the methylaminocarbene ion $\mathbf{2}^{\bullet+}$is an important reaction intermediate, and in particular, the lowest energy process from $\mathbf{1}^{\bullet+}$ is isomerization into $\mathbf{2}^{\bullet+}$ followed by elimination of a hydrogen atom to generate N-protonated methyl cyanide. Formation of the latter is confirmed by tandem mass spectrometry experiments and proton transfer between $[\mathbf{1} - H]^+$ ions and several reference bases conducted in a Fourier transform mass spectrometer.

Introduction

Numerous studies have been devoted to the gas-phase chemistry of the vinyl alcohol radical cation $[CH_2{=}CHOH]^{\bullet+}$.[1] Particular attention has been paid to the low-energy process leading to a specific elimination of the hydroxyl hydrogen atom to produce the acetyl cation $[CH_3CO]^+$. The presently established conclusion, based on both experimental and theoretical arguments, is that the dissociation is preceded by a 1,2-hydrogen shift giving rise to ionized hydroxymethyl carbene $[CH_3{-}C{-}OH]^{\bullet+}$ and, thereby, to the fragments $[CH_3CO]^+ + H^\bullet$.

In contrast, the isoelectronic species, ionized vinylamine $[CH_2{=}CHNH_2]^{\bullet+}$ ($\mathbf{1}^{\bullet+}$), has not been considered in detail although its behavior presents some close similarities with that of $[CH_2{=}CHOH]^{\bullet+}$. Accordingly, it is known that ions $\mathbf{1}^{\bullet+}$ of low internal energy undergo exclusive elimination of a hydrogen atom; moreover, deuterium-labeling experiments shows that the eliminated hydrogen originates specifically from the amino group.[2] Several relevant questions remain however unsolved: What is the structure of the $[C_2H_4N]^+$ fragment ion coming from $\mathbf{1}^{\bullet+}$? How does the $H^\bullet$ elimination occur, via a direct N–H bond cleavage or after a rearrangement process? In the latter case, what is the favored path among the various possibilities sketched in Scheme I?

We attempt to tackle these questions by investigating portions of the $[C_2H_5N]^{\bullet+}$ potential energy surface related to Scheme I with the aid of high-level molecular orbital calculations. In addition, mass spectrometric techniques have been employed to determine the dissociation energetics and the fragment ion structures associated with the reaction $\mathbf{1}^{\bullet+} \rightarrow [C_2H_4N]^+ + H^\bullet$.

Computational Details

Ab initio molecular orbital calculations were carried out with a local version of the GAUSSIAN 90[3] program. Geometries of the structures considered were initially optimized at the Hartree–Fock level of theory with the split-valence 3-21G basis set. Harmonic vibrational wavenumbers were computed at this level (HF/3-21G) in order to characterize the stationary points obtained and to estimate zero point vibrational energies (ZPE). Geometrical parameters of relevant stationary points (equilibrium and transition structures) were then refined using correlated wavefunctions at the second order Moller–Plesset perturbation theory (MP2) level with the dp-polarized 6-31G** basis set. Improved relative energies were subsequently obtained through calculations using MP2/6-31G** geometries and the larger 6-311++G** basis set (++ denotes a set of sp-diffuse functions on C and N and s-diffuse functions on H)[4] and with more complete incorporation of electron correlation, namely the full fourth-order perturbation theory (MP4SDTQ). For open-shell species, the unrestricted formalism (UHF, UMP4) has been employed. To account for the slow convergence of the UMP4 series, the spin contaminations present in the UHF references were also removed by applying a projection technique (PUHF, PUMP4).[5] Unless otherwise noted, the relative energies referred to in the text

Scheme I

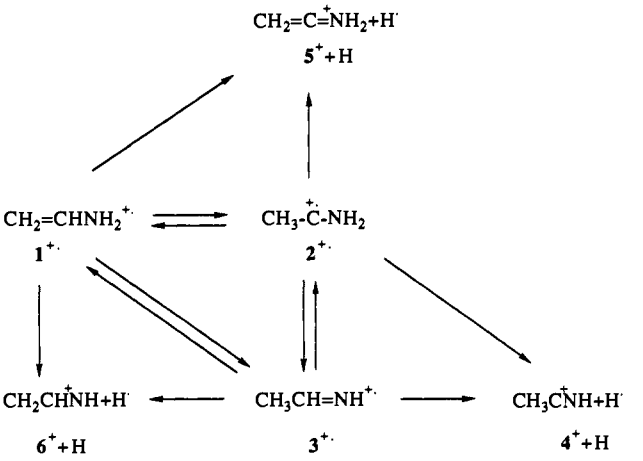

† Ecole Polytechnique.
‡ University of Leuven.
• Abstract published in *Advance ACS Abstracts,* October 15, 1993.

(1) Bouchoux, G. *Mass Spectrom. Rev.* **1988**, *7*, 1.
(2) Holmes, J. L.; Terlouw, J. K. *Can. J. Chem.* **1976**, *54*, 1007.
(3) *GAUSSIAN 90*; Gaussian Inc.: Pittsburg, PA, 1990.
(4) Frish, M. J.; Pople, J. A.; Binkley, J. S. *J. Chem. Phys.* **1984**, *80*, 3265.
(5) Schlegel, H. B. *J. Chem. Phys.* **1988**, *92*, 3075.

0002-7863/93/1515-9728$04.00/0

correspond to our best estimates obtained at the PUMP4/6-311++G**//MP2/6-31G**+ZPE level. At this level of theory an error of about ±15 kJ·mol^{-1} could be expected on heats of formation. Figures 1–3 display geometrical parameters of the various equilibrium and transition structures optimized at the MP2/6-31G** level for the purpose of this work. Corresponding total and relative energies are recorded in Tables I–III.

Experimental Section

The reactions of metastable ions were studied with a VG.Micromass ZAB 2F mass spectrometer. Mass analyzed ion kinetic energy (MIKE) spectra were obtained by selecting and focusing the ion of interest into the second field-free region of the mass spectrometer and scanning the electric sector voltage. Collision induced dissociation (CID) spectra were obtained with the MIKE methodology and by introducing helium as target gas into the collision cell located in the second field-free region. The helium pressure indicated by the ionization gauge located above the diffusion pump in this region was 10^{-7} mbar.

Proton-transfer experiments were performed in a Bruker CMS-47X Fourier transform ion cyclotron resonance (FT-ICR) spectrometer equiped with an external ion source. The ions $[C_2H_4N]^+$, formed by dissociative ionization of cyclobutylamine in the external ion source (typical conditions were filament current 3 A, ionizing voltage 30 V) and transferred to the ICR cell, were allowed to react with various bases for 0.5 s at a pressure of c.a. 10^{-7} mbar following ejection of the undesirable ions. Thermalization of $[C_2H_4N]^+$ ions was ensured by introducing argon into the ICR cell to a pressure of c.a. 10^{-6} mbar.

Results And Discussion

(1) Stable C_2H_5N and $[C_2H_5N]^{\bullet+}$ Isomers. The three radical cations **1**$^{\bullet+}$, **2**$^{\bullet+}$, and **3**$^{\bullet+}$ displayed in Figure 1 represent local minima on the $[C_2H_5N]^{\bullet+}$ surface, and our data confirm the results of Lien and Hopkinson obtained at the lower HF/6-31G*//HF/4-31G level.[6] Vinylamine radical cation $[CH_2{=}CHNH_2]^{\bullet+}$ (**1**$^{\bullet+}$) is the most stable isomer lying 81 and 122 kJ·mol^{-1} below ionized methylaminocarbene $[CH_3CNH_2]^{\bullet+}$ (**2**$^{\bullet+}$) and etheneimine $[CH_3CHNH]^{\bullet+}$ (**3**$^{\bullet+}$),respectively (Tables I and II). A heat of formation of 826 ± 5 kJ·mol^{-1} has been recently deduced for ionized vinylamine **1**$^{\bullet+}$ from a measurement of the threshold energy of $[C_2H_5N]^{\bullet+}$ ion formation from cyclobutylamine by photoionization experiment.[7] The heat of formation of **3**$^{\bullet+}$ can be deduced from the heat of formation of the neutral molecule, i.e. $\Delta H°_f$ (**3**) = 24 kJ·mol^{-1},[8] and its adiabatic ionization energy, IE(**3**) = 9.6 eV.[9] One thus obtains $\Delta H°_f$ (**3**$^{\bullet+}$) = 950 kJ·mol^{-1} with an error of about 10 kJ·mol^{-1} and, consequently, an experimental energy difference of 124 ± 15 kJ·mol^{-1} between **1**$^{\bullet+}$ and **3**$^{\bullet+}$, in close agreement with calculations.

The stability ordering of the neutral counterparts **1**, **2**, and **3** is in contrast with respect to their molecular cations (Table III). The most stable neutral is etheneimine **3**; isomers **1** and **2** are higher in energy by 22 and 148 kJ·mol^{-1}, respectively (a comparable difference in energy of 17 kJ·mol^{-1} between **1** and **3** has been calculated at the MP4/6-311+G**//HF/6-31+G**+ZPE level).[10] Only indirect determinations of the experimental heats of formation of **1** and **3** are available. For vinylamine, combination of its adiabatic ionization energy[11,12] and the heat of formation of its molecular cation leads to $\Delta H°_f$ (**1**) = 35 ± 10kJ·mol^{-1}. In the case of etheneimine a value of $\Delta H°_f$(**3**) = 24 ± 8kJ·mol^{-1} has been deduced from deprotonation enthalpy and heat of formation of the $[CH_3CHNH_2]^+$ cation.[8]

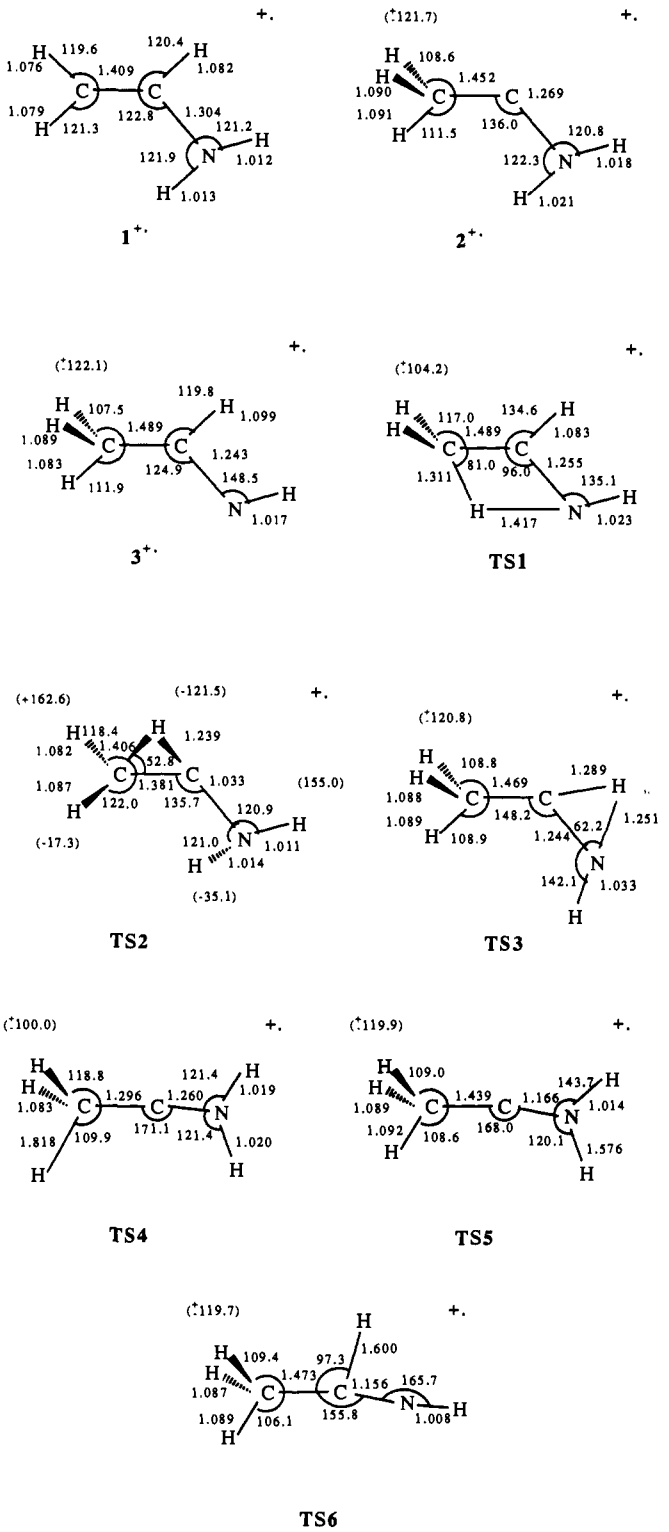

Figure 1. UMP2/6-31G**-optimized geometries of the $[C_2H_5N]^{\bullet+}$ equilibrium (**1**$^{\bullet+}$–**3**$^{\bullet+}$) and transition structures (TS1–TS6). Bond distances are given in Å and bond angles in degrees.

Thus, experiment points to a slightly higher stability of etheneimine with respect to vinylamine, and this tendency is confirmed by calculations.

Comparison of the geometries of the radical cations (Figure 1) and neutrals (Figure 3) gives information on the origin of the electron removed during ionization. The lengthening of the CC bond from **1** to **1**$^{\bullet+}$, accompanied by the shortening of the CN bond and the planarity of the nitrogen indicates a π-electron ionization; the electronic wave function of **1**$^{\bullet+}$ has in fact a $^2A''$

(6) Lien, M. H.; Hopkinson, A. C. *Can. J. Chem.* **1984**, *62*, 922.
(7) Bouchoux, G.; Alcaraz, C.; Dutuit, O. Unpublished results.
(8) Peerboom, R. A.; Ingeman, S.; Nibbering, N. M. M.; Liebman, J. F. *J. Chem. Soc., Perkin Trans. 2* **1990**, 1825.
(9) Lias, S. G.; Bartmess, J. E.; Liebman, J. F.; Holmes, J. L.; Levin, R. D.; Mallard, W. G. *J. Phys. Chem. Ref. Data* **1988**, *17*, Supplement No. 1.
(10) Smith, B. J.; Radom, L. *J. Am. Chem. Soc.* **1992**, *114*, 36.
(11) Albrecht, B.; Allan, M.; Haselbach, E.; Neuhaus, L.; Carrupt, P. A. *Helv. Chim. Acta* **1984**, *67*, 220.
(12) Lafon, C.; Gonbeau, D.; Pfister-Guillouzo, G.; Lasne, M.; Ripoll, J. L.; Denis, J. M. *Nouv. J. Chim.* **1986**, *10*, 69.
(13) Wurtehwein, E. U. *J. Org. Chem.* **1984**, *49*, 2971.

Table I. Calculated Total (hartree) and Zero-Point (kJ/mol) Energies for the $[C_2H_5N]^{\bullet+}$ Structures and $[C_2H_4N]^+$ Fragments

structure[a]		(U)MP2(F)/ 6-31G**[b]	(U)MP4SDTQ/ 6-311++G**[c]	(PU)MP4SDTQ/ 6-311++G**[d]	ZPE[e]	νi[f]	$\langle S^2\rangle$[g]
$1^{\bullet+}$	$^2A''$	−133.255 34	−133.335 11	−133.339 38	194.3		0.820
$2^{\bullet+}$	$^2A'$	−133.225 46	−133.305 33	−133.307 53	191.7		0.781
$3^{\bullet+}$	$^2A'$	−133.200 85	−133.285 09	−133.289 57	183.9		0.814
TS1	$^2A'$	−133.138 56	−133.223 94	−133.231 18	172.4	2386*i*	0.827
TS2	$^2A'$	−133.161 54	−133.244 61	−133.246 24	177.9	1856*i*	0.771
TS3	$^2A'$	−133.133 04	−133.216 81	−133.219 36	168.6	2796*i*	0.865
TS4	$^2A'$	−133.130 92	−133.213 65	−133.222 67	166.2	874*i*	0.881
TS5	$^2A'$	−133.142 14	−133.225 91	−133.235 78	163.0	1261*i*	0.923
TS6	$^2A'$	−133.152 09	−133.236 66	−133.244 49	162.2	1580*i*	0.882
4^+	$^1A_1$	−132.683 28	−132.757 74		161.3		
5^+	$^1A'$	−132.651 59	−132.728 70		163.9		
6^+	$^1A'$	−132.573 45	−132.653 94		158.1		
7^+	$^1A_1$	−132.668 51	−132.742 01		162.1		
8^+	$^1A_1$	−132.652 45	−132.728 10		161.5		

[a] Based on (U)MP2/6-31G** geometries. [b] Using full sets of MOs. [c] The core orbitals are frozen. Energy of H• is −0.4990 hartree. [d] Energies with spin projection. [e] Zero-point vibrational energy from (U)HF/3-21G calculations. [f] Imaginary frequencies (in cm^{-1}) of transition structures. [g] $\langle S^2\rangle$ in UHF references.

Table II. Relative Energies (kJ/mol) of the $[C_2H_5N]^{\bullet+}$ Stationary Points

structure	UMP2/ 6-31G**	UMP4/ 6-311++G**	PUMP4/ 6-311++G**	PUMP4 + ZPE[a]
$1^{\bullet+}$	0	0	0	0
$2^{\bullet+}$	86	78	84	81
$3^{\bullet+}$	143	131	131	122
TS1	307	292	284	265
TS2	246	238	245	230
TS3	321	311	315	292
TS4	327	319	306	281
TS5	297	287	272	244
TS6	271	258	249	220
$4^+ + H^\bullet$	215	206	217	187
$5^+ + H^\bullet$	299	282	293	266
$6^+ + H^\bullet$	504	478	489	457

[a] Including PUMP4/6-311++G** relative energies and ZPEs. The latter are the HF/3-21G values scaled by 0.9 to account for the systematic overestimation of vibrational frequencies at the HF level.

Table III. Calculated Total (hartree), Zero-Point, and Relative (kJ/mol) Energies of the Relevant Neutral C_2H_4N and C_2H_3N Species[a]

species	MP4SDTQ/ 6-311++G**[b]	ZPE[c]	ΔE[d]
1	−133.627 90	192.8	0
2	−133.579 80	192.0	126
3	−133.636 50	193.0	−22
9	−132.452 44	129.6	0
10	−132.413 35	127.8	101
11	−132.401 62	124.9	129

[a] Based on MP2/6-31G** geometries. [b] Core orbitals are frozen. [c] At the HF/3-21G level and scaled by 0.9. [d] Relative energies corrected for zero-point contribution.

symmetry. Another important point to mention is that the radical site is essentially located on the terminal carbon and the positive charge is distributed among all hydrogen atoms and the central carbon. Ionization of methylaminocarbene **2** is accompanied by a slight decrease in the CC and CN bond lengths and by an opening of the CCN bond angle (from 109.9° to 136.0°). In $2^{\bullet+}$, the spin density and positive charge are mostly located on the central carbon atom, thus pointing toward an ionization on the carbene site. Ion $3^{\bullet+}$ is produced by removal of an electron from the nitrogen lone pair; the main consequence of the ionization process is an opening of the CNH bond angle (from 109.4° to 148.5°).

Finally, ionization energy values may be briefly discussed. We report in Table IV adiabatic and vertical ionization energies of **1**–**3** calculated at the MP4/6-311++G**//MP2/6-31G**+ZPE level. Comparison with experiment is only possible for **1** and **3** that were prepared by flash thermolysis and studied by photoelectron spectroscopy.[11,12] A systematic underestimation of c.a. 0.2–0.3 eV is in fact expected from calculations at this level of theory.

Table IV. Calculated and Experimental Ionization Energies of Species **1**–**3**[a]

species	IEa exp	IEa calc[b]	IEv exp	IEv calc[b]
1	8.20[c]	7.9	8.65[c]	8.41
2		7.4		8.07
3	9.6[d]	9.4	10.25[d]	10.24

[a] In eV. [b] At the PUMP4/6-311++G**//MP2/6-31G**+ZPE level. [c] References 12 and 13. [d] Reference 13.

(2) Stable $[C_2H_4N]^+$ Isomers and Their Conjugate Bases C_2H_3N. Five $[C_2H_4N]^+$ structures were examined including three potential products of H•-elimination from $1^{\bullet+}$–$3^{\bullet+}$ (Scheme I), i.e. cations 4^+–6^+ and two other candidates predicted to be stable in earlier studies,[14-16] $[CH_3NCH]^+$ (7^+), and $[CH_2{=}N{=}CH_2]^+$ (8^+). Their energies are summarized in Table I whereas their structures are displayed in Figure 2.

Present calculations confirm the order of stability established at the lower HF/6-31G*//3-21G level.[14] The protonated methyl cyanide $[CH_3CNH]^+$ (4^+) is again found to be the most stable structure. The four other isomers, namely $[CH_3NCH]^+$ (7^+), $[CH_2NCH_2]^+$ (8^+), $[CH_2CNH_2]^+$ (5^+), and $[CH_2CHNH]^+$ (6^+) are situated at 42, 78, 79, and 270 kJ·mol^{-1}, respectively, above 4^+ (values at the MP4/6-311++G**//MP2/6-31G**+ZPE level). Comparison with known heats of formation is possible only for 4^+ and 7^+. Our calculated relative energy of 42 kJ·mol^{-1} is in pleasant agreement with the experimental difference in $\Delta H°_f$ of 43 kJ·mol^{-1}.

Three neutral molecules, corresponding to the conjugate bases of ions 4^+–8^+ have also been examined at the same level of theory (Table III, Figure 3). We find methyl isocyanide CH_3NC (**10**) to be less stable than methyl cyanide CH_3CN (**9**) by 101 kJ·mol^{-1}. This energy difference is very close to the difference in heats of formation of these two species, i.e. 99 kJ·mol^{-1}.[9] The third neutral structure, $CH_2{=}C{=}NH$ (**11**) is calculated to lie 129 kJ·mol^{-1} above **9**.

These results allow the proton affinities (PAs) of the C_2H_3N isomers to be estimated (Table V). Protonation of **9** and **11** giving 4^+ and 7^+, respectively, has been considered as well as protonation of $CH_2{=}C{=}NH$ (**10**) at its three possible basic sites. It is clear in the latter case that protonation at the terminal

(14) Nguyen, M. T.; Ha, T. K. *J. Chem. Soc., Perkin Trans. 2* **1984**, 1401.
(15) DeFrees, D. J.; McLean, A. D.; Herbst, E. *Astrophys. J.* **1985**, *293*, 236.
(16) Koyanagi, G. K.; Wang, J.; March, R. E. *Rapid Commun. Mass Spectrom.* **1990**, *4*, 373.

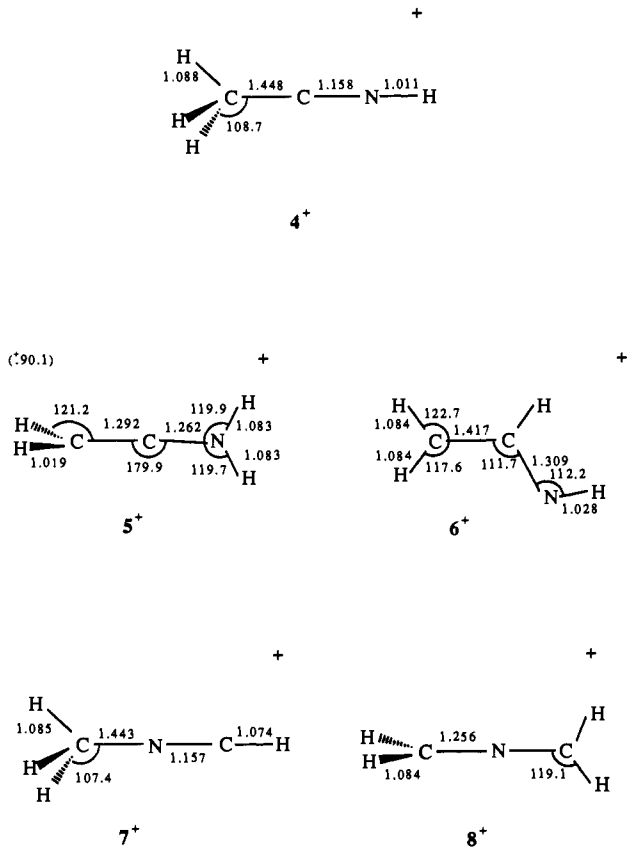

Figure 2. MP2/6-31G**-optimized geometries of the $[C_2H_4N]^+$ structures (4^+–8^+). Bond distances are given in Å and bond angles in degrees.

carbon atom is largely favored.[14] Comparison between computation and experiment reveals for **9** and **11** a slight underestimation of 12–15 kJ·mol^{-1} on absolute PA by calculation, but then relative PA is satisfactorily reproduced (56 kJ·mol^{-1}, experiment; 59 kJ·mol^{-1}, calculation). The reliability of the calculated proton affinities presented in Table V provides a mean to distinguish ionic structures 4^+–6^+. The deprotonation enthalpies of these ions are clearly different: 773 kJ·mol^{-1} for 4^+ (giving **9**), 823 kJ·mol^{-1} for 5^+, and 632 kJ·mol^{-1} for 6^+. We will make use of these large differences to characterize the structure of the $[C_2H_4N]^+$ ion coming from $1^{\bullet+}$, as will be seen below.

(3) Isomerization and Dissociation of $[C_2H_5N]^{\bullet+}$ Ions. As indicated in Scheme I, the three considered entities $1^{\bullet+}$–$3^{\bullet+}$ may undergo several rearrangement processes involving 1,2- or 1,3-hydrogen migrations. Such reactions, in analogous systems, are known to possess high energy barriers. Indeed, the three rearrangements corresponding to the transition structures TS1, TS2, and TS3 require critical energies in the range 170–265 kJ·mol^{-1}. A schematic potential energy profile showing the unimolecular rearrangement processes connecting $1^{\bullet+}$, $2^{\bullet+}$, and $3^{\bullet+}$ and their dissociation reactions is presented in Figure 4. Calculated relative energies are included in Table II.

Starting from $1^{\bullet+}$ two isomerization channels are opened. Our calculations predict that rearrangement of ionized vinylamine $1^{\bullet+}$ to ionized methylaminocarbene $2^{\bullet+}$ (TS2, a 1,2-hydrogen migration) exhibits a smaller barrier (by 35 kJ·mol^{-1}) than rearrangement to ionized ethenimine $3^{\bullet+}$ (TS1, a 1,3-hydrogen migration). The second access to $3^{\bullet+}$, i.e. isomerization of $2^{\bullet+}$ by 1,2-hydrogen migration (TS3) needs a further 62 kJ·mol^{-1} with respect to TS2. Considering now the dissociation routes, it appears that the transition structure TS5 for H$^\bullet$ loss from $2^{\bullet+}$ lies below TS1 and TS3 by 21 and 48 kJ·mol^{-1}, respectively. Thus hydrogen atom elimination from $2^{\bullet+}$ is energetically favored over rearrangement into $3^{\bullet+}$, and consequently the lowest energy dissociation route for ionized vinylamine is $1^{\bullet+} \rightarrow$ TS2 $\rightarrow 2^{\bullet+} \rightarrow$ TS5 $\rightarrow 4^+ + H^\bullet$. Since calculation indicates that TS5 is 14 kJ·mol^{-1} higher in energy than TS2, the rate determining step during $1^{\bullet+} \rightarrow 2^{\bullet+} \rightarrow 4^+ + H^\bullet$ is predicted to be the final N–H bond elongation. Overall, calculations suggest the formation of $[CH_3CNH]^+$ (4^+) as the most abundant product from $1^{\bullet+}$.

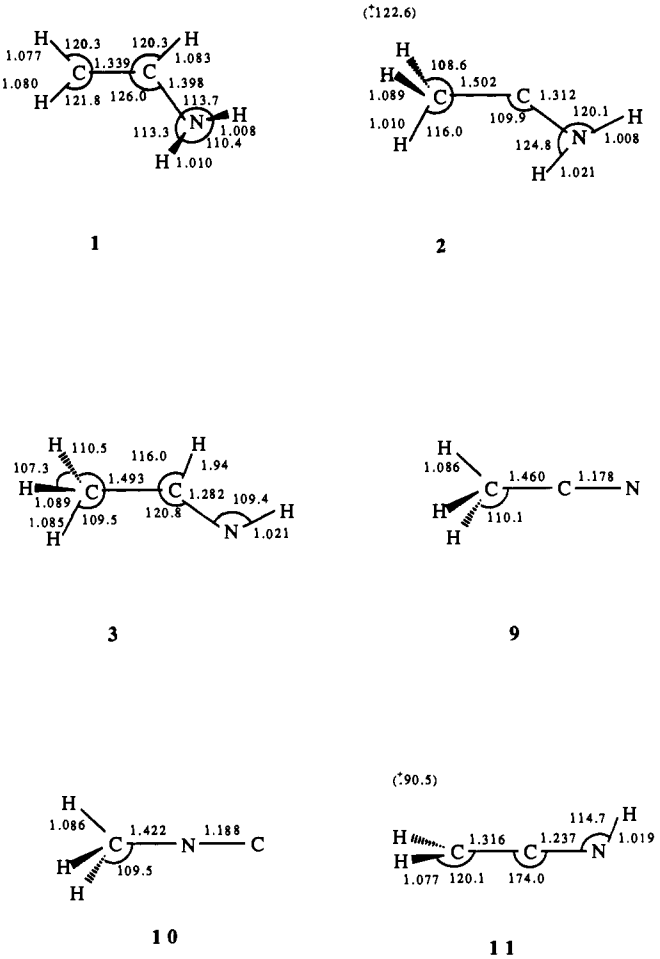

Figure 3. MP2/6-31G**-optimized geometries of the neutral $[C_2H_5N]$ (**1**–**3**) and $[C_2H_3N]$ (**9**–**11**) structures. Bond distances are given in Å and bond angles in degrees.

Table V. Calculated and Experimental Proton Affinity Values[a]

species[b]	PA (calc)	PA (exp)[c]
9 CH_3CN (4^+)	773	788
10 CH_2CNH (5^+)	823	
10 CH_2CNH (4^+)	902	
10 CH_2CNH (6^+)	632	
11 CH_3NC (7^+)	832	844

[a] The calculated proton affinity refers to $E[C_2H_4N]^+ - E(C_2H_3N)$ estimated using MP4/6-311++G**//MP2/6-31G**+ZPE values and expressed in kJ·mol^{-1}. [b] In parentheses are protonated structures $[C_2H_4N]^+$ considered. [c] Reference 9.

(4) Comparison with Mass Spectrometric Results. It has been concluded from an earlier mass spectrometric study[2] that the vinylamine radical cation $1^{\bullet+}$ is purely formed by dissociative ionization of cyclobutylamine:

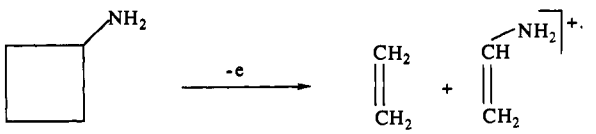

We therefore used this procedure to generate ions $1^{\bullet+}$ in the sources of the VG ZAB 2F and Bruker CMS 47X mass spectrometers.

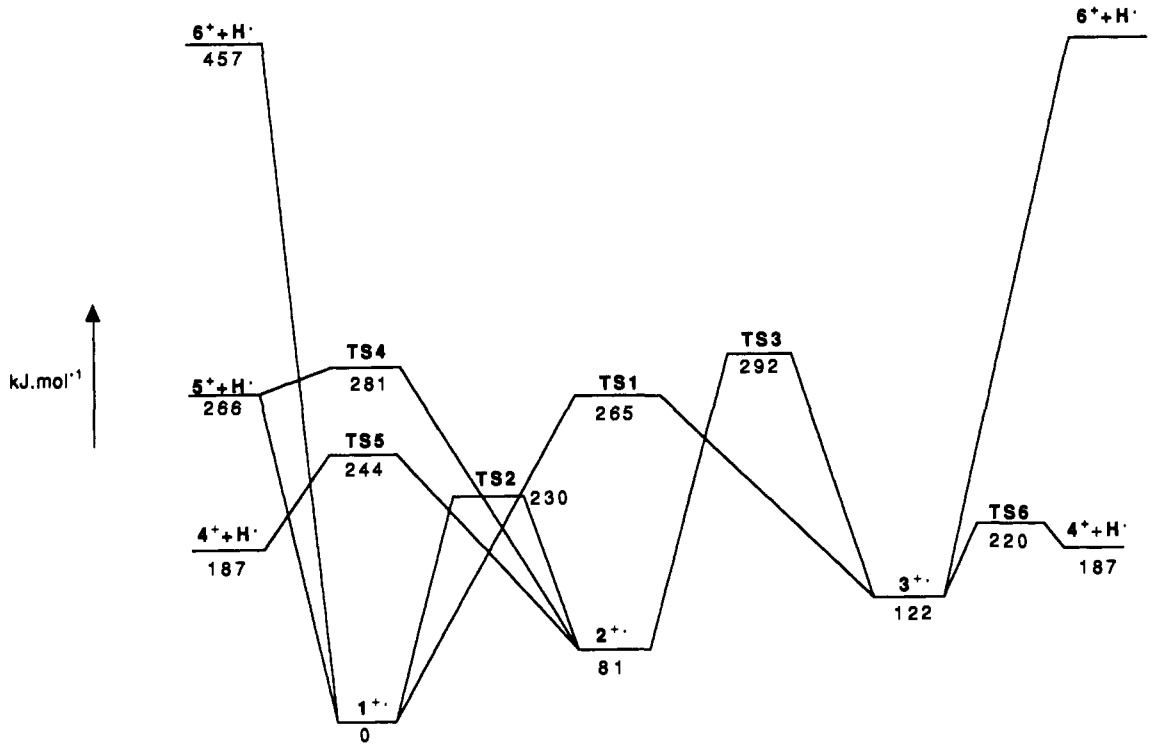

Figure 4. Schematic potential energy profiles for unimolecular rearrangements among $[C_2H_5N]^{\bullet+}$ isomers ($\mathbf{1}^{\bullet+}$–$\mathbf{3}^{\bullet+}$) and H-loss processes. Values obtained at the (PU)MP4/6-311++G**//MP2/6-31G**+ZPE level.

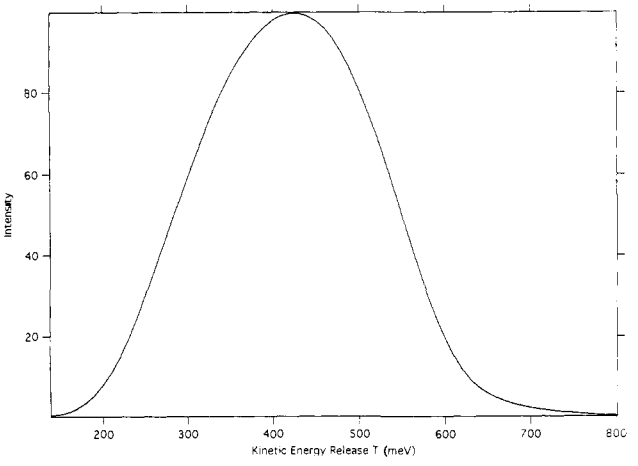

Figure 5. Experimental kinetic energy release distribution for the dissociation $[CH_2{=}CHNH_2]^{\bullet+} \rightarrow [C_2H_4N]^+ + H^{\bullet}$.

Our MIKE experiments show that unimolecular dissociation of metastable ions $\mathbf{1}^{\bullet+}$ consists exclusively in the loss of one H• atom. The metastable transition $\mathbf{1}^{\bullet+} \rightarrow [C_2H_4N]^+ + H^{\bullet}$ is associated with a dish-topped peak from which a kinetic energy release distribution $n(T)$ has been derived by an analytical treatment.[16] The result presented in Figure 5 shows a one-component distribution pointing toward the occurrence of only one reaction process. As usually noted for a dished-topped peak, the most probable T value (425 meV) is very close to the $T_{0.5}$ value (410 meV) determined from the measurement of the peak width at half height. Thus, for metastable dissociations of isotopomers of $\mathbf{1}^{\bullet+}$, we report only the latter values in Table VI.

Deuterated ion $[CH_2{=}CHND_2]^{\bullet+}$ ($\mathbf{1}^{\bullet+}$) looses exclusively a deuterium atom with the release of a slightly higher amount of kinetic energy (430 meV). Interestingly enough, when isotopomer $[CH_2{=}CHNHD]^{\bullet+}$ is sampled, two dissociation channels are opened and intramolecular isotope effect is clearly observed in both peak intensities and kinetic energy release T. The abundance ratio (H loss)/(D loss) is equal to 4.9 in our experiments whilst the ratio $(T_{\text{H loss}})/(T_{\text{D loss}})$ is equal to 1.12 with a T difference of 50 meV. These observations confirm those of Holmes and Terlouw,[2] who examined the fragmentation of $\mathbf{1}^{\bullet+}$ occurring in the first field-free region of an AEI MS 902 instrument. Small differences are however evident due to the difference in observation time between the two experiments. In the MIKE methodology we sample ions of longer lifetime and, consequently, of lower internal energy. Isotope effect is expected to increase with decreasing internal energy; accordingly the abundance ratio (H loss)/(D loss) is greater in the MIKE spectrum (4.9) than in the experiment described in ref 2 (3.9).

Table VI. Characteristics of X• (X = H or D) Loss from Metastable $[CH_2{=}CHNX_2]^{\bullet+}$ Ions[a]

species	X	% abundance[b]	$T_{0.5}$ (meV)[c]
$[CH_2{=}CHNH_2]^{\bullet+}$	H	100	410
$[CH_2{=}CHNHD]^{\bullet+}$ [d]	H	83	400
$[CH_2{=}CHNHD]^{\bullet+}$ [d]	D	17	450
$[CH_2{=}CHND_2]^{\bullet+}$ [d]	D	100	430

[a] MIKE experiments. [b] Based on peak area. [c] After correction for the main beam width. [d] Ions obtained after deuteration of the cyclobutylamine by D_2O exchanges in the inlet system of the mass spectrometer.

We turn now to the question of the structure of the $[C_2H_4N]^+$ fragment ion produced by dissociation of $\mathbf{1}^{\bullet+}$. Two kinds of experiments demonstrate that it is protonated acetonitrile $[CH_3CNH]^+$ ($\mathbf{4}^+$).

Firstly, the MIKE and CID-MIKE spectra of $[\mathbf{1}\text{-}H^{\bullet}]^+$ are identical to those of $[CH_3CNH]^+$ ions produced under chemical ionization conditions. The two major unimolecular dissociations of both ions attested by the MIKE spectra are (i) loss of H (70% abundance, $T_{0.5} = 83 \pm 5$ meV) and (ii) $[CH_3]^+$ production (30% abundance, $T_{0.5} = 10 \pm 2$ meV; the latter characteristics agree with the data reported in refs 17 and 18). Collisional activation of $[\mathbf{1}\text{-}H^{\bullet}]^+$ and $[CH_3CNH]^+$ ions leads to the CID-MIKE spectra which exhibit clear similarities, as illustrated in Figure 6.

(17) Iraki, M.; Lifshitz, C. *Int. J. Mass Spectrom. Ion Processes* **1986**, *71*, 245.
(18) Wincel, H.; Fokkens, R. H.; Nibbering, N. M. M. *Int. J. Mass Spectrom. Ion Processes* **1989**, *88*, 241.

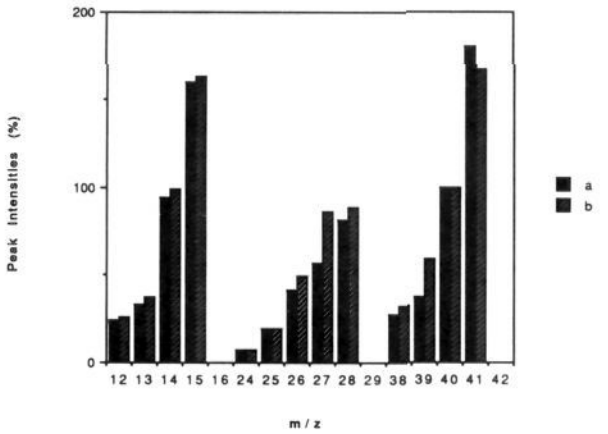

Figure 6. Histogram representation of the CID spectra of $[C_2H_4N]^+$ ions from (a) electron ionization of cyclobutylamine and (b) ammonia chemical ionization of acetonitrile (peak heights

Table VII. Observation of Proton Transfer from $[C_2H_4N]^+$ Ions Originating from Cyclobutylamine to References Bases B

B	PA(B)[a]	proton transfer
propene	751	–
bromobenzene	763	–
acetaldehyde	781	±
cyclohexene	791	+
acetic acid	795	+
ethyl cyanide	806	+

[a] Proton affinity values (kJ·mol^{-1}) from ref 9.

Another way of probing an ion structure is to use specific ion–molecule reactions. Deprotonation is an important, structure specific and characteristic reaction for this purpose. Preceding calculations have shown that deprotonation enthalpies of $[C_2H_4N]^+$ ions **4**$^+$–**6**$^+$ are quite different (Table V); thus if we are are able to attain experimentally the deprotonation enthalpy of $[\mathbf{1}\text{-H}^\bullet]^+$ ions, we can identify its structure. Proton-transfer reactions 1

$$[\mathbf{1}\text{-H}^\bullet]^+ + B \rightarrow C_2H_3N + BH^+ \qquad (1)$$

where B is a reference base having known proton affinity have been consequently studied in an FT-ICR spectrometer. The results are reported in Table VII. From the occurrence or nonoccurrence of reaction 1, a deprotonation enthalpy of 780 ± 10 kJ·mol^{-1} can be deduced for $[\mathbf{1}\text{-H}^\bullet]^+$ ions. Returning to the PA estimates associated with the neutrals **9**–**11** (Table V), it is clear that only acetonitrile (**9**) is consistent with the above value and that, consequently, $[CH_3CNH]^+$ ion is the ionic product of dissociation of **1**$^{\bullet+}$.

Observation of a favored elimination of the light isotope H$^\bullet$ from $[CH_2{=}CHNHD]^{\bullet+}$ ions implies that the rate-determining step involves the departing H or D. In our reaction scheme, this means that the step **2**$^{\bullet+} \rightarrow$ **4**$^+$ + H$^\bullet$ is the most energy consuming. This conclusion is in agreement with calculations which place the corresponding transition structure TS5 14 kJ·mol^{-1} above the TS2 of the 1,2-H migration **1**$^{\bullet+} \rightarrow$ **2**$^{\bullet+}$. The dissociative step **2**$^{\bullet+}$ $\rightarrow$ **4**$^+$ + H$^\bullet$ is associated with a reverse critical energy of 57 kJ.mol^{-1}. The existence of such a large reverse critical energy is attested by the observation of an important kinetic energy released during the fragmentation (Figure 5 and Table VI). We also note that a major part of this energy is recovered in the kinetic energy released during the fragmentation (425 meV i.e. 41 kJ·mol^{-1}) and this demonstrates a nonstatistical distribution of the vibrationnal energy during the separation of the fragments **4**$^+$ and H$^\bullet$. As indicated by labeling experiments, the loss of H$^\bullet$ occurs specifically from the amino group; no mixing of these hydrogen atoms with the two other positions is observed, and consequently reversible isomerization reactions such as **1**$^{\bullet+} \leftrightarrow$ **3**$^{\bullet+}$ and **2**$^{\bullet+} \leftrightarrow$ **3**$^{\bullet+}$ must be excluded. This, combined with the demonstration that the fragment ion structure is $[CH_3CNH]^+$, shows that the behavior of low-energy vinylamine radical cations is restricted to the reaction path **1**$^{\bullet+} \rightarrow$ **2**$^{\bullet+} \rightarrow$ **4**$^+$ + H$^\bullet$. Strong kinetic effect participates in this situation favoring the reaction **1**$^{\bullet+} \rightarrow$ **2**$^{\bullet+}$ over reaction **1**$^{\bullet+} \rightarrow$ **3**$^{\bullet+}$ because the former possesses the lowest critical energy and the highest "frequency factor" (TS2 is less hindered than TS1). Similarly, direct dissociation from **2**$^{\bullet+}$ into **4**$^+$ + H$^\bullet$ is associated with a lower critical energy and a higher frequency factor than the reaction **2**$^{\bullet+} \rightarrow$ **3**$^{\bullet+}$.

Concluding Remarks

In summary we find that (i) neutral etheneimine $CH_3CH{=}NH$ (**3**) is more stable than vinylamine $CH_2{=}CHNH_2$ (**1**) and methylaminocarbene CH_3CNH_2 (**2**) by 22 and 148 kJ·mol^{-1}, respectively; (ii) ionized vinylamine **1**$^{\bullet+}$ lies 81 kJ·mol^{-1} below ionized methylaminocarbene **2**$^{\bullet+}$ and 122 kJ·mol^{-1} below ionized etheneimine **3**$^{\bullet+}$; (iii) specific loss of one H atom from the amino group of **1**$^{\bullet+}$ to produce protonated methyl cyanide is attested by tandem and Fourier transform mass spectrometry experiments; and (iv) the minimum-energy reaction path for ionized vinylamine is **1**$^{\bullet+} \rightarrow$ **2**$^{\bullet+} \rightarrow$ $[CH_3CNH]^+$ + H$^\bullet$, the last step being rate determining and responsible for the large amount of energy released during the fragmentation.

Acknowledgment. M.T.N. is indebted to the Belgian National Fund for Scientific Research (NFWO) and the Belgian Government (DPWB).